Monte Carlo Molecular Modeling Studies of Hydrated Li-, Na-, and K-Smectites: Understanding the Role of Potassium as a Clay Swelling Inhibitor

E. S. Boek,*,† P. V. Coveney,† and N. T. Skipper‡

Contribution from Schlumberger Cambridge Research, High Cross, Madingley Road, Cambridge CB3 0EL, England, and Department of Physics and Astronomy, University College, London WC1E 6BT, England

Received June 29, 1995[⊗]

Abstract: Monte Carlo molecular modeling simulations have been performed to investigate some of the microscopic mechanisms underlying smectite clay swelling. The systems we have studied represent hydrated Wyoming montmorillonites in which the counterions are Li^+, Na^+, or K^+. For each of these three counterions we have conducted a series of 15 simulations in which the water content is increased systematically from 0 to 300 mg/g of clay. In this paper we introduce a new set of interaction potentials that can be used to study clay−water−cation systems and which lend themselves to future studies of intercalated organic molecules. We compare simulation data for the clay layer spacing with experimental swelling curves and find that the level of agreement is striking. Interestingly, in regions where the experimental curves exhibit hysteresis for adsorption/desorption, these loops enclose our calculated data. This indicates that our simulations indeed represent states of thermodynamic equilibrium, conditions which are harder to achieve experimentally. We are therefore content with our choice of atomistic interaction potentials for the current work. Analysis of the microscopic interlayer structure reveals a qualitative difference between Li^+ and Na^+ on the one hand and K^+ on the other. We find that as the water content is increased, both Li^+ and Na^+ are able to hydrate, thereby becoming detached from the clay surface. In contrast, we find that K^+ ions migrate to and bind to the clay surface during our simulations. Therefore K^+ ions screen the negatively charged, mutually repelling clay surfaces more effectively than Na^+ and Li^+ ions do. The reluctance of K^+ ions to fully hydrate will reduce the tendency of K^+-saturated clays to expand. Our simulations therefore provide a qualitatively satisfying insight into the role of K^+ ions as a clay swelling inhibitor. Indeed, the differences between Na^+ and K^+ ions displayed in these simulations may also be of more general relevance to colloid chemistry and physiology.

1. Introduction

Swelling clay minerals play an important role in many industrial processes, such as petroleum engineering and catalysis. During oil and gas exploration and production, serious problems are frequently encountered in shale formations, which contain a high fraction of compacted 2:1 clay minerals such as smectites. These problems include borehole instability, associated with the uptake of water by smectites from the drilling fluid.

Smectites are comprised of layers of negatively charged mica-like sheets held together by charge-balancing counterions such as Na^+ and Ca^{2+}. In the presence of water these cations tend to hydrate, thereby forcing the clay layers apart in a series of discrete steps.[1,2] A number of studies claim that the sorption of water into the interlayer spacing is mainly determined by the size and charge of the counterions;[1,3] other authors have shown that the net silicate layer charge[4] and charge location[5] play a major role. At increasing relative humidity, smectites adsorb water vapor and form one-, two-, and three-layer hydrates.[2,4,6] Cases *et al.* have found that the swelling process of sodium montmorillonite was isoenthalpic beyond the two-layer hydration state.[6] Low *et al.* on the other hand still observed a decrease of the heat of immersion beyond this state.[7,8] A number of experiments have yielded insight into the molecular distribution and organization of interlayer water and cations adsorbed on clay surfaces;[9] these include X-ray,[10,11] infrared,[12] and neutron diffraction[13,14] studies. Nevertheless, the microscopic structure of water and the distribution of counterions near the clay−water interface is still a controversial subject in colloid science: the question as to what extent counterions hydrate in the interlamellar space is still unresolved. Sposito and Prost[9] claim that counterion solvation plays a dominant role in the swelling of clays, whereas Low[15] attributes swelling to hydration of the clay surfaces.

* Address correspondence to this author at the following E-mail address: boek@cambridge.scr.slb.com.

† Schlumberger Cambridge Research.

‡ University College.

⊗ Abstract published in *Advance ACS Abstracts,* December 1, 1995.

(1) Mooney, R. W.; Keenan, A. G.; Wood, L. A. *J. Am. Chem. Soc.* **1952**, *74*, 1367−1371.

(2) Brindley, G. W.; Brown, G. *Crystal Structures of Clay Minerals and their X-ray Identification*; Mineralogical Society: London, 1980; Chapter 3.

(3) Keren, R.; Shainberg, I. *Clays Clay Miner.* **1975**, *23*, 193−200.

(4) Suquet, H.; de la Calle, C.; Pezerat, H. *Clays Clay Miner.* **1975**, *23*, 1−9.

(5) Sato, T.; Watanabe, T.; Otsuka, R. *Clays Clay Miner.* **1992**, *40*, 103−113.

(6) Cases, J. M.; Bérend, I.; Besson, G.; François, M.; Uriot, J. P.; Thomas, F.; Poirier, J. E. *Langmuir* **1992**, *8*, 2730−2739.

(7) Zhang, Z. Z.; Low, P. F. *J. Colloid Interface Sci.* **1989**, *133*, 461−472.

(8) Fu, M. H.; Zhang, Z. Z.; Low, P. F. *Clays Clay Miner.* **1990**, *38*, 485−492.

(9) Sposito, G.; Prost, R. *Chem. Rev.* **1982**, *82*, 553−573.

(10) Pezerat, H.; Méring, J. *C. R. Seances Acad. Sci. Ser. D* **1967**, *265*, 529−532.

(11) Ben Brahim, J.; Besson, G.; Tchoubar, C. *J. Appl. Crystallogr.* **1984**, *17*, 179−188.

(12) Sposito, G.; Prost, R.; Gaultier, J.-P. *Clays Clay Miner.* **1983**, *31*, 9−16.

(13) Skipper, N. T.; Soper, A. K.; McConnell, J. D. C. *J. Chem. Phys.* **1991**, *94*, 5751−5760.

(14) Skipper, N. T.; Soper, A. K.; Smalley, M. V. *J. Phys. Chem.* **1994**, *98*, 942−945.

(15) Low, P. F. *Langmuir* **1987**, *3*, 18−25.

0002-7863/95/1517-12608$09.00/0

Two types of swelling should be distinguished in relation to clay hydration: (1) *intracrystalline* swelling, involving the adsorption of limited amounts of water in the interlayer spacing, and (2) *osmotic* swelling, related to unlimited adsorption of water due to the difference between ion concentrations close to the clay surface and in the pore water. The mechanisms of intracrystalline swelling have been described above; osmotic swelling gives rise to macroscopic expansion of the clay. The tendency of *sodium*-saturated smectites to swell macroscopically is the principal cause of shale instability in drilling operations and may even lead to collapse of the wellbore. The worldwide cost of wellbore instability problems to the oil industry is estimated to be more than $600 million per year. For this reason, a large research effort has been directed to shale-swelling inhibition. Oil-based drilling fluids do not cause shale swelling, as they exclude additional water from the wellbore. Such fluids, however, are environmentally unacceptable and are particularly hazardous to marine ecosystems. Therefore current research in this field is focused at improving the properties of water-based drilling muds. One route of action is the development of biodegradable polymer additives for the drilling mud. The additive molecules are considered to adsorb preferentially onto the clay particles, thereby displacing water molecules. Another method for inhibition of shale swelling is the addition of weakly hydrating cations, such as K^+, to the drilling fluid.[16] The potassium ion will replace sodium by cation exchange within the clay and is found to prevent swelling. Unfortunately, this treatment requires high concentrations of KCl, which is environmentally toxic. Nevertheless, an understanding of the microscopic mechanisms of cation hydration in relation to clay swelling can contribute to the design of new additives for water-based muds, which may even be active in the absence of potassium ions.

At large interlamellar distances (>20 Å), the stability of colloidal clay suspensions is well described by the DLVO theory.[17,18] This continuum theory fails at smaller interlamellar distances; in this regime the structure of the solvent must be considered explicitly at the molecular level.[19] This is particularly the case for potassium smectite clays: the DLVO theory assumes that the balancing counterions are detached from the clay surface, forming a diffuse double layer. As will be shown in this study, this approach is not valid for potassium ions since they tend to stick to the clay surface. The microscopic mechanisms underlying clay swelling are controlled by the structure and dynamics of water and counterions at the clay–water interface. In general, the properties of a liquid near a solid interface are different from those of the bulk liquid. Experiments have shown that the interaction with a solid surface induces layering in the confined liquid, thereby changing its structural and dynamical properties.[19] Computer simulations of aqueous solutions near solid surfaces have confirmed this picture: they show strong oscillations of the water density at the surface, lateral positional and orientational ordering of the adsorbed water molecules,[20,21] and a decreased mobility of interface water molecules compared to those within the bulk liquid.[22,23] In the case of hydrated smectites, microscopic information from *e.g.* neutron diffraction experiments is inaccessible, since smectites only occur as small platelets (typically 5 μm^2).[24] Under these circumstances, computer simulations can provide new insights at the molecular level. The philosophy behind these statistical mechanical simulations is to construct a mathematical model of interactions described by potential functions, followed by sampling of the configurational space of a many-particle system to determine its equilibrium properties.[25] In recent years, a number of Monte Carlo (MC) and molecular dynamics (MD) simulations on clay–water–cation systems have been published by Skipper *et al.*[24,26–28] and Refson *et al.*[29] In the course of this work, Skipper *et al.* have developed a model framework for smectite–hydrates which is small and therefore computationally efficient but still representative of the macroscopic system. Delville has performed MC simulations of smectite–water systems[30–32] and the clay–vapor interface.[33] Both authors found good (semi)quantitative agreement between simulation results and experimental and/or thermodynamic data.

In the present paper, we investigate the swelling of smectite clays at the molecular level, using the Monte Carlo simulation technique developed by Skipper. In the systems studied, the counterions are Li^+, Na^+, or K^+. For each of the three cations, the water content is increased stepwise in a series of 15 simulations from 0 to 300 mg/g of clay. This has allowed us to monitor the intracrystalline expansion of smectite clays, almost up to the onset of osmotic swelling. By comparing the hydration behavior of the three cations, it is our goal to obtain microscopic insight into why, broadly speaking, sodium and lithium smectites swell macroscopically but potassium smectites do not.

Our present work is different from the previously mentioned work in a number of respects, which we want to clarify here. First, we have used a new set of interaction potentials to study the clay–water–cation systems. The validity of these potentials is tested by comparing calculated interlayer spacings to experimentally measured swelling curves. An advantage of this potential set is that it can be used in combination with organic molecules. Second, we have conducted simulations in which the counterions are Li^+, Na^+, and K^+, whereas the work of Skipper *et al.* has been concerned with the behavior of Na^+ and Mg^{2+} ions.[24] Third, by increasing the water content in small steps, we are able to obtain detailed insight into the variation of the interlayer spacing and molecular structure with changing water content. Fourth, our work complements the calculations of Delville, who has studied similar systems[30–32] but using different statistical mechanical ensembles and potential functions and a two-dimensional structure model for the smectite hydrates. Having established the potential model and molecular swelling

(16) Denis, J. H.; Keall, M. J.; Hall, P. L.; Meeten, G. H. *Clay Miner.* **1991**, *26*, 255–268.
(17) Verwey, E. J. W.; Overbeek, J. T. G. *Theory of the Stability of Lyophobic Colloids*; Elsevier: New York, 1948.
(18) Derjaguin, B.; Landau, L. D. *Acta Physicochim. URSS* **1941**, *14*, 635.
(19) Israelachvili, J. N. *Intermolecular and Surface Forces*; Academic Press: London, 1985.
(20) Spohr, E. *J. Phys. Chem.* **1989**, *93*, 6171–6180.
(21) Liu, X. Y.; Boek, E. S.; Briels, W. J.; Bennema, P. *Nature* **1995**, *374*, 342–345.
(22) Raghavan, K.; Foster, K.; Motakabbir, K.; Berkowitz, M. *J. Chem. Phys.* **1991**, *94*, 2110–2117.
(23) Boek, E. S.; Briels, W. J.; van Eerden, J.; Feil, D. *J. Chem. Phys.* **1992**, *96*, 7010–7018.
(24) Skipper, N. T.; Refson, K.; McConnell, J. D. C. *J. Chem. Phys.* **1991**, *94*, 7434–7445.
(25) Allen, M. P.; Tildesley, D. J. *Computer Simulation of Liquids*; Clarendon, Press: Oxford, 1987.
(26) Skipper, N. T.; Chang, F.-R. C.; Sposito, G. *Clays Clay Miner.* **1995**, *43*, 285–293.
(27) Skipper, N. T.; Sposito, G.; Chang, F.-R. C. *Clays Clay Miner.* **1995**, *43*, 294–303.
(28) Chang, F.-R. C.; Skipper, N. T.; Sposito, G. *Langmuir.* **1995**, *11*, 2734–2741.
(29) Refson, K.; Skipper, N. T.; McConnell, J. D. C. In *Geochemistry of Clay-Pore Fluid Interactions*; Manning, D. C., Hall, P. L., Hughs, C. R., Eds.; Chapman and Hall; London, 1993; p 1.
(30) Delville, A. *Langmuir* **1991**, *7*, 547–555.
(31) Delville, A. *Langmuir* **1992**, *8*, 1796–1805.
(32) Delville, A. *J. Phys. Chem.* **1993**, *97*, 9703–9712.
(33) Delville, A.; Sokolowski, S. *J. Phys. Chem.* **1993**, *97*, 6261–6271.

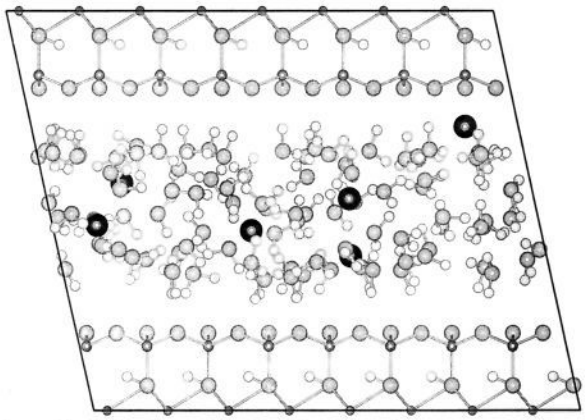

Figure 1. Molecular model of sodium Wyoming montmorillonite as used in the Monte Carlo simulations. The simulation cell consists of two montmorillonite layers (upper and lower part of the figure), 6 sodium ions (black), and 96 water molecules (middle part of the figure).

mechanisms, future studies on the action of intercalated organic shale-swelling inhibitor molecules will be possible.

We believe that our present work may be of wider relevance than solely to the study of clays. The difference between the hydration properties of potassium and sodium ions in the vicinity of solid−liquid interfaces is crucial in a number of fields: the outcome of many colloidal and also physiological processes is determined by a subtle balance between the tendencies of each cation to hydrate or to adsorb at a macromolecular surface.

2. Simulation Methods and Potential Models

Our choice of simulation methods and potential models is driven by the following requirements. (1) The ability to reproduce experimental thermodynamic data, such as interlayer spacing and potential energies. Having verified these, we may seek to calculate the microscopic interlayer structure. (2) The possibility of simulating smectite swelling under wellbore conditions, requiring adjustment of the interlayer spacing with increasing pressure. For this purpose we have used a constant (NpT) ensemble, in which the pressure p is applied normal to the clay layers. (3) The possibility of including organic molecules for future shale inhibition applications.

We will now discuss the models and methods used.

2.1. Structure Model of the Clay Sheet. The model clay mineral studied is a Wyoming-type montmorillonite, with the unit cell formula

$$M_{0.75}[Si_{7.75}Al_{0.25}](Al_{3.5}Mg_{0.5})O_{20}(OH)_4$$

where M represents a monovalent cation: in the present work Na^+, K^+, and Li^+ are considered. This prototypical swelling clay mineral is a member of the smectite family[34] and consists of two tetrahedral layers, sandwiching an octahedral layer (2:1). Figures 1 and 2 show molecular models of hydrated Na- and K-Wyoming montmorillonites, respectively. One out of eight Al atoms in the octahedral network is substituted by a Mg atom. Likewise, one out of 32 Si atoms in the tetrahedral sheet is replaced by an Al atom. These substitutions are typical for a Wyoming-type montmorillonite[34] and give rise to an overall negative charge on the clay framework. This negative charge is balanced by the presence of monovalent interlayer counterions M. The effect of the two types of substitution is different: the negative charge, associated with tetrahedral layer substitution, can be distributed over just the three surface oxygens of one tetrahedron. This means that the liquid in the interlayer spacing experiences a localized negative charge, giving rise to strong complexation of water and cations. The liquid feels a much more diffuse negative charge associated with the octahedral (layer) substitution, as this charge can distribute itself over more oxygen atoms.[35] Thus it is not surprising that the swelling properties of smectite clays depend in a subtle way on the character of the isomorphic substitutions.[2] In order to model a Wyoming montmorillonite in a realistic way, it is therefore important to employ a representative substitution scheme. In previous simulations of montmorillonite−water interfaces, only tetrahedral substitutions of Si by Al were taken into account.[30−32] Following the nomenclature,[34] this type of clay should rather be considered as a beidellite, which has different swelling properties.[2]

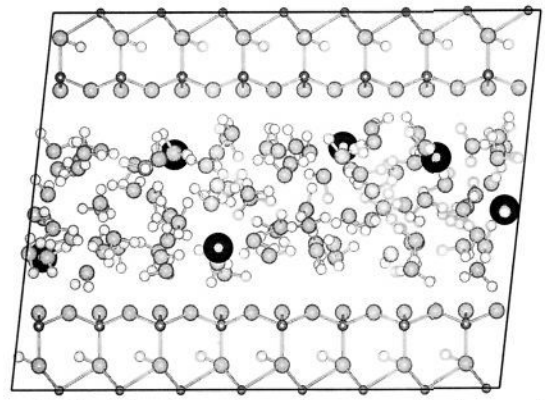

Figure 2. Simulation image of potassium montmorillonite, containing 6 potassium ions (black) and 96 water molecules.

2.2. Monte Carlo Simulations. Our Monte Carlo (MC) simulations were performed using the computer program MONTE,[36] as described by Skipper *et al.*[24] This code, which uses the Metropolis algorithm,[25,37] has been designed primarily to simulate molecular liquids (*e.g.* water and aqueous solutions) between solid surfaces. Liquid molecules are treated as rigid bodies, and molecular orientations are stored as quaternions. Our periodic simulation cell consists of two opposing Wyoming montmorillonite layers measuring 21.12 × 18.28 Å^2, equivalent to eight unit cells. The thickness of one layer is 3.28 Å. Periodic boundary conditions are applied in three dimensions. Skipper *et al.*[26] have found evidence that the properties of our relatively small simulation cell are still representative of the macroscopic system and are not influenced by artificial long-range symmetry of the imposed periodic lattice. In view of the 3D periodic boundary conditions, the simulations model an infinite stack of clay platelets, very similar to a real clay mineral. Two-dimensional periodic boundary conditions, as applied in previous simulations,[30−33] would not seem to be particularly useful for the modeling of clay minerals, as the octahedral layer substitutions at the box boundaries cannot be correctly represented.[26] van der Waals interactions are treated within an all-image regime,[25] with a cut-off radius of 9 Å. Long-range electrostatic interactions are calculated by using the Ewald sum method[25] in conjunction with three-dimensional periodic boundary conditions. In this way, long-range interactions are correctly treated, which is essential for a reliable calculation of equilib-

(34) Newman, A. C. D. *Chemistry of Clays and Clay Minerals*; Mineralogical Society: London, 1987; Chapter 1.

(35) Sposito, G. *The Surface Chemistry of Soils*; Oxford University Press: New York, 1984; Chapters 1 and 2.

(36) Skipper, N. T. *MONTE User's Manual*; Department of Physics and Astronomy, University College London, 1993.

(37) Metropolis, N.; Rosenbluth, A. W.; Rosenbluth, M. N.; Teller, A. H.; Teller, E. *J. Chem. Phys.* **1953**, *21*, 1087−1092.

rium counterion distributions.[38] Our simulations were performed in the isothermal−isobaric (NpT) ensemble, more strictly a constant ($N\sigma T$) ensemble, in which a uniaxial stress σ_{zz} of 10^5 Pa was applied perpendicular to the clay layers. The volume of the system is allowed to vary, and the simulation will predict the layer spacing. The temperature was fixed at $T = 300$ K. Ideally, the chemical potential μ of the system would be kept constant during the simulation, rather than the number of particles N. However, satisfactory equilibration in such a grand ensemble simulation is computationally difficult to achieve for liquid water. In his grand canonical (μVT) simulations, Delville[30−33] judged equilibration to have taken place after a comparatively small number of steps; other authors prescribe for liquid water a much larger number of MC moves to achieve a truly equilibrated state, in which insertion and deletion of molecules have equal probability.[39] Therefore we have chosen to keep the number of water molecules and cations constant.

A Monte Carlo move involves a change in the center of mass coordinates and the orientation of a randomly selected molecule. Moves involving a change in the layer spacing are attempted with a lower probability (typically 20%). The simulation cell was allowed to change shape as well, so that adjacent clay layers may registrate. The general probability of acceptance of a move is

$$P = \min\{1, \exp(-\Delta H/kT)\} \quad (1)$$

where

$$\Delta H = U_n - U_m + \sigma_{zz}(V_n - V_m) - NkT \ln (V_n/V_m) \quad (2)$$

ΔH is the enthalpy change in moving from initial state m to final state n, U is the corresponding potential energy, and V is the volume.

At the start of each simulation, the water molecules were placed at random within the interlayer region and the cations were placed in two planes at 7.5 Å from the centers of both clay layers. Equilibration was judged to have taken place when the average potential energy and the z-dimension of the simulation cell had reached constant values. This typically took 250 000 moves. The simulations were then allowed to proceed for at least another 2 million steps, which required a calculation time of approximately 48 CPU hours on an IBM RS/6000 workstation. Data were collected every 1000 attempted steps. From these data, averaged potential energies, layer spacings, interlayer atomic density profiles, radial distribution functions, and orientations of the interlayer water molecules were calculated.

2.3. Model Interaction Potentials. The quality of MC and MD simulations is highly dependent on the choice of the interaction potentials;[26] particularly in the case of hydrated smectite clays, the total interaction energy contains many terms, which are all in a subtle balance.[30−33] Building on the experience of previous models, in this paper we propose a new, more flexible set of interaction potentials that can be used to study smectite hydrates.

The water−water interaction was simulated using the empirical TIP4P model of Jorgensen *et al.*[40] In this model, the water molecule is rigid and has four intermolecular interaction sites. Interactions are pairwise additive, involving Coulombic and Lennard-Jones 6−12 potential terms:

$$v(r) = \sum_{ij}(q_i q_j/r_{ij} - D_{ij}/r_{ij}^6 + E_{ij}/r_{ij}^{12}) \quad (3)$$

Charges are assigned to the hydrogen atoms and to a massless site M on the C_2 axis, located 0.15 Å away from the oxygen atom toward the hydrogen atoms. The fourth site is the neutral oxygen atom, which is the only van der Waals interaction site. Advantages of the TIP4P model compared to the MCY model,[41] which has been used in previous clay−water simulations,[26,27] are the facts that the TIP4P model (1) is compatible with the OPLS force field for organic molecules[42] (this creates the possibility of including intercalated organic molecules in future shale inhibition simulations) and (2) gives the correct liquid water density at 300 K and 0.1 MPa pressure, whereas the MCY model requires a pressure of 850 MPa to maintain a density of 1.0 g cm^{-3}.[43] In a previous study,[26] the MCY model was found to describe the behavior of 2:1 Na−clay mineral interlayers slightly better than the TIP4P model; in the present paper we want to investigate the properties of the TIP4P model in relation to smectite layers saturated with Li^+, Na^+, and K^+ counterions at varying water contents.

The water−cation interactions we used are compatible with the water−water TIP4P potential. For both Na^+ and Li^+, parameters were taken from Jorgensen *et al.*,[44] as these are incorporated in the OPLS force field.[42] They are conveniently represented by Coulombic and Lennard-Jones terms (see Tables 1 and 2, respectively). For K^+, however, parameters from the same source were unavailable. We have considered three available interaction potentials to represent the K^+−H_2O interactions. In order to test these potentials, we have performed simulations of dehydrated K-montmorillonites and used the resulting interlayer spacing as a judgement criterion. K^+ potentials taken from Åqvist[45] and Wipff *et al.*,[46] both having the Lennard-Jones 6−12 functional form, give layer spacings of 11.2 and 11.6 Å, respectively, which deviate strongly from the experimental value of 10.1 Å.[47] This indicates that the cation−clay interactions are not well represented in either of these potential sets. Parameters taken from Bounds[48] on the other hand, based on *ab initio* calculations for cation−TIP4P water complexes, give a value of 9.9 Å. Because of this good agreement we chose Bounds' K^+−H_2O potential for all subsequent simulations. In this model, the local charges on the water molecule are the same as in the TIP4P model, and the van der Waals interactions is represented by the sum of potassium−hydrogen soft repulsions

$$v_{KH}(r) = A_{KH} \exp(-b_{KH} r) \quad (4)$$

and a potassium−oxygen attractive−repulsive contribution

$$v_{KO}(r) = A_{KO} \exp(-b_{KO} r) - C_{KO}/r^4 + D_{KO}/r^6 \quad (5)$$

In contrast with the Lennard-Jones potential, the r^{-6} term is repulsive, but is compensated by the attractive r^{-4} term, which is related to charge-induced dipole interactions. The latter term

(38) Bleam, W. F. *Rev. Geophys.* **1993**, *31*, 51−73.
(39) Cracknell, R. F.; Nicholson, D.; Parsonage, N. G.; Evans, H. *Mol. Phys.* **1990**, *71*, 931−943.
(40) Jorgensen, W. L.; Chandrasekhar, J.; Madura, J. D.; Impey, R. W.; Klein, M. L. *J. Chem. Phys.* **1983**, *79*, 926−935.
(41) Matsouka, O.; Clementi, E.; Yoshimine, M. *J. Chem. Phys.* **1976**, *64*, 1351−1361.
(42) Briggs, J. M.; Matsui, T.; Jorgensen, W. L. *J. Comput. Chem.* **1990**, *11*, 958−971.
(43) Skipper, N. T.; McConnell, J. D. C.; Refson, K. In *Recent Developments in the Physics of Fluids, International Symposium, Oxford*, Institute of Physics, 1991, F269−F276.
(44) Chandrasekhar, J.; Spellmeyer, D. C.; Jorgensen, W. L. *J. Am. Chem. Soc.* **1984**, *106*, 903−910.
(45) Åqvist, J. *J. Phys. Chem.* **1990**, *94*, 8021−8024.
(46) Wipff, G.; Weiner, P.; Kollman, P. *J. Am. Chem. Soc.* **1982**, *104*, 3249−3258.
(47) Calvet, R. *Ann. Agron.* **1973**, *24*, 77−133.
(48) Bounds, D. G. *Mol. Phys.* **1985**, *54*, 1335−1355.

Table 1. Local Electronic Charges, As Used in Eq 3

site	$q(e)$	site	$q(e)$
M (H_2O)	−1.04	Li, Na, K	1.0
H (H_2O, OH)	0.52	Si	1.2
O (surface)	−0.8	Al (tetr)	0.2
O (OH)	−1.52	Al (oct)	3.0
O (apical)	−1.0	Mg	2.0

Table 2. van der Waals Parameters, As Used In Eqs 3, 4, and 5

sites	A (kcal/mol)	$b \times 10^{-2}$ (Å^{-1})	C (kcal Å^4/mol)	D (kcal Å^6/mol)	$E \times 10^{-3}$ (kcal Å^{-12}/mol)
Na^+-Na^+				300.0	14.0
Li^+-Li^+				100.0	0.4
O−O				610.0	600.0
$O-Li^+$				247.0	15.5
$O-Na^+$				427.8	91.7
$O-K^+$	538.84	3.339	438.0	638.0	
K^+-H	57.47	3.4128			
K^+-Si	0.19	0.749			
K^+-Al	0.19	0.749			

is expected to be more important for puffier ions such as K^+ and is possibly responsible for the good agreement between the calculated and observed layer spacing. Preliminary results indicate that qualitatively similar results are obtained when Bounds' 4−6 potential function is fitted to a Lennard-Jones 6−12 functional form.

Interaction potentials between the clay mineral and water molecules or cations have been obtained from semiempirical cluster calculations.[30-32] Such calculations however do not yield reliable parametres for short-range van der Waals interactions,[41] which are important in hydrogen-bonded systems, such as interlayer water. We have employed potentials for the interactions with the clay mineral, developed according to a method described by Skipper *et al.*[26] In our model, the clay surface oxygen atoms are represented by TIP4P (water) oxygen atoms. In this way optimal use is made of the potentials already mentioned for water−water[40] and water−cation[44] interactions. The interaction potential has been extended with structural OH groups, apical oxygen atoms, and tetrahedral (Si, Al) and octahedral (Al, Mg) cations. All charges used are listed in Table 1, while all van der Waals parameters are given in Table 2. Although this approach also involves significant approximations, Skipper *et al.* have found good agreement between experimental data and simulations based on this method.[27,28]

3. Results and Discussion

We performed three series of simulations, which cover Li-, Na-, and K-Wyoming montmorillonites. Each series consisted of 15 simulations, with water contents varying from 0 to 96 water molecules. This was done in steps of four molecules (from 0 to 16) or eight molecules (from 16 to 96 molecules). For montmorillonites, 0 to 96 water molecules correspond to 0 to *ca.* 300 mg/g of clay, which are values typically encountered experimentally, when dry clays are allowed to absorb water from the vapor phase.[8] We will first present results for the calculated thermodynamic properties of the clay−hydrates. Having verified these, we will focus on the microscopic structure of the interlayer.

3.1. Thermodynamic Properties. Simulation results for the thermodynamic properties of the interlayer water molecules in the Li-, Na-, and K-Wyoming montmorillonites are presented in Tables 3 and 4. In Table 3 the water contents and potential energies are listed; in Table 4 the interlayer spacings and macroscopic interlayer densities are given.

3.1.1. Potential Energies. The potential energy $\Delta U(N)$ of interlayer water was calculated as a function of increasing water content:

$$\Delta U(N) = \frac{U(N) - U(0)}{N} \tag{6}$$

where $U(N)$ equals the potential energy of the total system, containing N water molecules. $U(0)$ is the potential energy of the anhydrous clay. This function is shown for all three clay hydrates in Figure 3. During the first stage of hydration, the Li− and Na−clay hydrate energies drop to levels significantly below the value for the internal energy of bulk TIP4P water, *i.e.* 42.27 ± 0.07 kJ mol^{-1}.[49] In the case of the K-clay on the other hand, $\Delta U(N)$ decreases less rapidly, initially having values above the bulk water energy. This means that during the first stages of clay swelling, it is energetically favorable for water molecules to invade the anhydrous Li- and Na-clay, whereas water molecules should be repelled from the K-clay. From a kinetic point of view, therefore, anhydrous Na- and Li-smectites are more inclined to swell than K-smectites. Once the initial energy barrier has been taken, the energy values for the K curve drop to the same level as the Na and Li curves.

After the initial decrease of the three energy functions, minima are reached, beyond which the curves rise again with increasing water content. In contrast to results from clay simulations using MCY water,[28] the value for bulk water is not yet reached at the highest water content for any of the three cations. This result is in agreement with experimental data of Fu *et al.*,[8] who still found a decrease of the heat of immersion beyond this water content.

3.1.2. Swelling Curves. The interlayer spacings of Li-, Na-, and K-montmorillonites have been calculated as a function of water content increasing from 0 to 96 molecules. In total, 15 points along these curves have been calculated, yielding a detailed picture of the swelling behavior of the different clays at low water content. These curves are shown in Figures 4, 5, and 6, respectively.

The curve for Na-smectite is shown in Figure 4, together with experimental isotherms obtained by Fu *et al.*[8] and Calvet.[47] In our calculated curve, the variation of the layer spacing with water content takes place in a monotonic, though stepwise manner. There is a gradual increase in the layer spacing at low water content (0−8 H_2O molecules), then a jump occurs going up to 12 H_2O molecules, followed by a gradual build up of the first water layer which is completed when 48 H_2O molecules are present. A justification at the molecular level for the formation of discrete water layers will be given in the next section. Then there is another sharp step in the layer spacing between 48 and 56 H_2O molecules, after which a second water layer begins to form. The layer spacing for water contents around this water layer transition region fluctuates strongly, even after 3 million MC equilibration steps, indicative of the transition from monolayer to bilayer water structure. Intriguingly, the experimental curve obtained by Fu *et al.*[8] shows two branches, surrounding our simulated swelling curve at these points, due to hysteresis: the interlayer spacing diverges upon evaporation or condensation of water vapor, the technique used by these authors to vary the water content of the pore. Our interpretation is that our simulated curve represents the true quasi-static equilibrium path for the transition from a monolayer to a bilayer situation. For more details, see ref 56. Upon further hydration, the second water layer gradually builds up, in close agreement with Fu's experimental results. After the addition of 88 water molecules, our calculated curve diverges from the curve by Fu, coinciding with the stepwise start of a new water layer. From

(49) Jorgensen, W. L.; Madura, J. D. *Mol. Phys.* **1985**, *56*, 1381−1392.

Table 3. Thermodynamic Properties of Hydrated Li^+-, Na^+-, and K^+-Montmorillonites: Water Content and $\Delta U(N)$

	water content (mg/g of clay)			$\Delta U(N)^a$ (kJ mol^{-1})		
no. of water molecules	Li^+	Na^+	K^+	Li^+	Na^+	K^+
0	0.0	0.0	0.0	0.00	0.00	0.00
4	12.6	12.0	12.0	−66.65 (5.23)	−71.34 (5.65)	−27.74 (5.23)
8	25.1	24.5	24.0	−63.93 (3.26)	−67.32 (3.31)	−46.36 (3.05)
12	37.6	36.7	36.1	−74.89 (2.64)	−65.90 (2.43)	−55.31 (2.43)
16	50.1	49.0	48.2	−75.35 (2.22)	−66.23 (2.01)	−57.99 (1.80)
24	75.2	73.4	72.2	−69.33 (1.55)	−60.79 (1.59)	−61.76 (1.46)
32	100.2	98.0	96.3	−62.34 (1.30)	−57.99 (1.21)	−60.08 (1.26)
40	125.3	122.3	120.4	−58.32 (1.42)	−55.31 (1.17)	−59.58 (1.09)
48	150.4	147.0	144.5	−57.15 (2.76)	−53.85 (0.92)	−58.07 (1.00)
56	175.4	171.3	168.5	−54.60 (1.00)	−50.50 (1.09)	−55.19 (1.00)
64	200.5	196.0	193.0	−52.59 (0.84)	−49.66 (0.88)	−51.76 (0.84)
72	225.5	220.0	217.0	−51.21 (0.88)	−49.62 (0.79)	−50.96 (0.75)
80	250.6	245.0	241.0	−51.13 (0.79)	−48.91 (0.79)	−49.96 (0.79)
88	275.5	269.0	265.0	−50.33 (0.75)	−47.99 (0.92)	−49.96 (0.63)
96	300.7	294.0	289.0	−49.50 (0.63)	−47.95 (0.92)	−49.29 (0.59)

[a] Potential energy per mole of interlayer water and standard deviation.

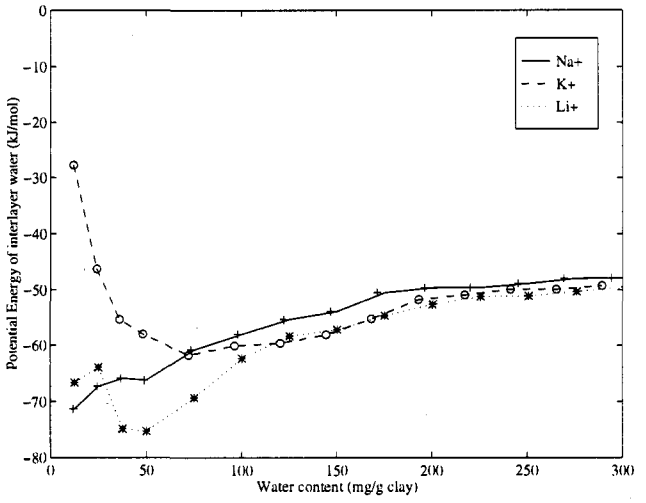

Figure 3. Potential energy of interlayer water in Na^+-, Li^+-, and K^+-Wyoming montmorillonites as a function of increasing water content, compared to the anhydrous state.

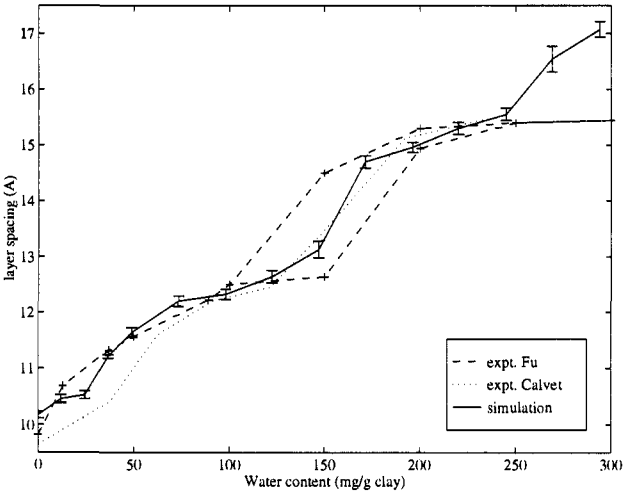

Figure 4. The interlayer spacing of Na^+-Wyoming montmorillonite as a function of increasing water content. The water content is expressed in terms of m_w/m_c, the mass ratio of water to Na^+-montmorillonite. Our simulation curve, represented as a solid line, consists of 15 measurements ranging from 0 to 96 water molecules, with increments in steps of 4 (from 0 to 16 water molecules) or 8 water molecules (from 16 to 96 water molecules). The measurements of the interlayer spacing were made as an average over a million iterations; the error bars represent rms deviations. In regions where the experimental curve, drawn as a dashed line, displays hysteresis for expansion/contraction, these loops enclose our calculated data.

this point on, the experimental layer spacing remains almost constant with increasing water content. This implies that, during these experiments, there was either an increase of the density or, more probably, condensation of water vapor on the exterior of the clay particle. In general, however, our calculated curve is in excellent agreement with Fu's experimental curve, indicating that our model and force fields are valid. In order to make a direct comparison with Fu *et al.*, the experimental vapor pressures should really be used in the simulations. However, we may expect that use of a fixed pressure of 10^5 Pa rather than the equilibrium pressure has very little effect on the layer spacing as the adsorbed water layer is presumably quite incompressible. We can illustrate this numerically by calculating the actual isothermal compressibility β_T of the water layer from volume fluctuations $\langle \delta V^2 \rangle$[25]

$$\beta_T = \langle \delta V^2 \rangle / V k_B T \tag{7}$$

where V is the volume of the water layer and cations only; as the clay layer itself is rigid, it does not contribute to the volume fluctuations. The fluctuations can be obtained from the rms deviations of the layer spacings, listed in Table 4. For 96 water molecules $\beta_T = 1.76 \times 10^{-10}$ Pa^{-1}, which is of the same order of magnitude as that for bulk water ($\beta_T = 4.57 \times 10^{-10}$ Pa^{-1}). As bulk water is quite incompressible, the same holds for clay interlayer water. In order to investigate this point more thoroughly, we have also performed simulations for the sodium smectite with 64 water molecules at the experimental vapor pressure of 2000 Pa. After 2 million steps, the layer spacing was found to be 14.95 ± 0.10 Å. Comparison with the layer spacing at 10^5 Pa (14.96 ± 0.09 Å; see Table 4) confirms that the effects on the layer spacing of using a fixed pressure of 10^5 Pa rather than the experimental equilibrium pressure are indeed negligible.

The Na curve measured by Calvet[47] almost coincides with our curve in the transition region from monolayer to bilayer structure. This curve was measured by evaporation of a clay suspension: apparently the dehydration process was performed more slowly than in Fu's experiments, in closer approximation to equilibrium conditions. Previous simulations of Na-smectite hydrates do not show stepwise swelling.[31] This discrepancy with experimental observations could have several explanations: first, the interlayer water density might not have converged to equilibrium during the grand canonical simulations; second, the short-range repulsions and hydrogen-bonding in-

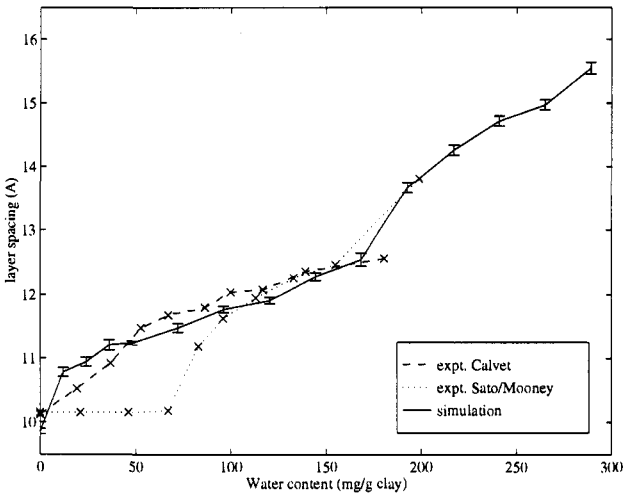

Figure 5. The interlayer spacing of K^+-Wyoming montmorillonite, as a function of increasing water content.

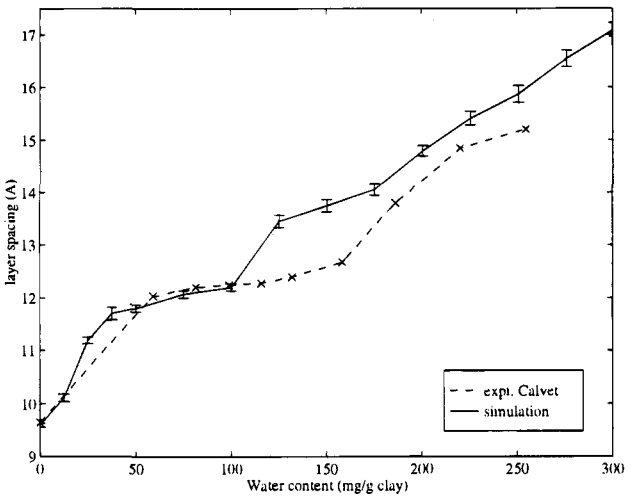

Figure 6. The interlayer spacing of Li^+-Wyoming montmorillonite, as a function of increasing water content. The experimental curve, drawn as a dashed line, represents the lower branch of a hysteresis loop.

Table 4. Thermodynamic Properties of Hydrated Li^+-, Na^+-, and K^+-Montmorillonites: Interlayer Spacing and $\Delta\rho(N)$

no. of water molecules	layer spacing[a] (Å)			$\Delta\rho(N)^b$ (g cm^{-3})		
	Li^+	Na^+	K^+	Li^+	Na^+	K^+
0	9.60 (0.04)	10.17 (0.06)	9.86 (0.04)	0.00	0.00	0.00
4	10.11 (0.07)	10.45 (0.07)	10.78 (0.07)	0.61	1.11	0.34
8	11.19 (0.06)	10.52 (0.07)	10.94 (0.07)	0.39	1.77	0.57
12	11.70 (0.12)	11.21 (0.03)	11.21 (0.08)	0.44	0.89	0.69
16	11.80 (0.07)	11.64 (0.09)	11.24 (0.03)	0.56	0.84	0.90
24	12.07 (0.07)	12.20 (0.09)	11.48 (0.07)	0.75	0.92	1.15
32	12.20 (0.07)	12.32 (0.09)	11.77 (0.05)	0.95	1.15	1.30
40	13.45 (0.12)	12.64 (0.11)	11.91 (0.05)	0.81	1.26	1.51
48	13.75 (0.12)	13.13 (0.15)	12.28 (0.06)	0.90	1.26	1.54
56	14.06 (0.11)	14.70 (0.11)	12.54 (0.10)	0.97	0.96	1.62
64	14.79 (0.10)	14.96 (0.09)	13.67 (0.08)	0.96	1.04	1.30
72	15.41 (0.13)	15.30 (0.11)	14.26 (0.08)	0.96	1.09	1.27
80	15.87 (0.16)	15.55 (0.11)	14.72 (0.08)	0.99	1.15	1.28
88	16.54 (0.16)	16.54 (0.23)	14.97 (0.08)	0.98	1.07	1.34
96	17.09 (0.13)	17.07 (0.14)	15.54 (0.09)	0.99	1.08	1.31

[a] Layer spacing (c-axis) and standard deviation. [b] Interlayer water density, calculated according to eq 7.

teractions, determining the packing of water molecules in the interlayer spacing, are inadequately represented.

The calculated curve for K-Wyoming smectite is given in Figure 5, together with an expansion curve obtained by Sato *et al.*[5] and an experimental evaporation curve obtained by Calvet.[47] The first experimental curve was measured as a function of water (mass) content, the latter curve was measured as a function of relative humidity (%), which was transformed to a function of water content by data obtained from Mooney *et al.*[1] In our calculated curve, there is a jump upon going from the anhydrous clay to clay containing four water molecules. Then the first water layer builds up and a further jump occurs at 64 molecules, when the second layer starts. Generally the jumps are less pronounced than for the sodium clay. At intermediate water content (100−200 mg/g of clay), our curve is in good agreement with Sato's curve and also reproduces the jump at 64 molecules. At low-hydration stages, our curve is significantly above the experimental one, which does not show any increase of the layer spacing with increasing water content up to 70 mg/g of clay. Again, this is probably due to preferential condensation of water on the exterior of the clay particles. Indeed, there is a rapid jump at the origin of the simulated curve, associated with only a small value of the hydration energy at that point (see Figure 3). This confirms our hypothesis of a high energetic barrier for initial hydration of the anhydrous K-smectite (see section 3.1.1). Comparison with Calvet's experiments shows excellent agreement over the whole measured range from 0−180 mg/g of clay. An explanation for this agreement may be that Calvet has dehydrated the clay, as opposed to Sato's adsorption experiments. In this way no activation energy barrier has to be overcome, related to the opening of the anhydrous clay. Calvet however considers K-montmorillonite to be a one (water) layer clay, while Na- and Li-smectites swell in two steps. Although it is possible to obtain larger layer spacings,[47,50] Calvet's experiments end at the monolayer stage. For higher water contents, we find that a second water layer starts, probably associated with another activation energy barrier. Indeed, the incremental potential energy of water in K-smectites, defined as the difference between $\Delta U(N)$ of two subsequent hydration states (not presented, but easily obtainable from $\Delta U(N)$) in Table 3), shows a local maximum at 64 water molecules. Furthermore, it should be noted that the layer spacing for a water content of 96 H_2O molecules (the last simulation data point) is considerably lower for K- than for Na-Wyoming smectite. This trend is in qualitative agreement with experimental data for various ions at constant relative humidity.[2]

The MC simulation curve for the lithium smectite is shown in Figure 6. This curve is compared with experimental data obtained by Calvet.[47] In general, the features of this curve are very similar to those of the sodium curve: a large jump occurs at the transition to the bilayer phase, at a somewhat lower water content than for the sodium case. It is remarkable that the experimental curve almost coincides with the simulated one at low water content. From 100 mg/g of clay, the two curves start to diverge, exactly at the point where, according to our calculations, the second water layer starts. The experimental curve was obtained by evaporation, probably representing the lower branch of a hysteresis loop.

3.1.3. Macroscopic Water Density. In order to focus on the stepwise swelling behavior, subtracting the linear increase of the interlayer spacing with water content, the density $\varrho(N)$ of the water interlayer was calculated as a function of water content

$$\varrho(N) = \frac{N m_{H_2O}}{V(N) - V(0)} \tag{8}$$

Here $V(N) - V(0)$ is the volume difference between a smectite

(50) Newman, A. C. D. *Chemistry of Clays and Clay Minerals*; Mineralogical Society: London, 1987; Chapter 5.

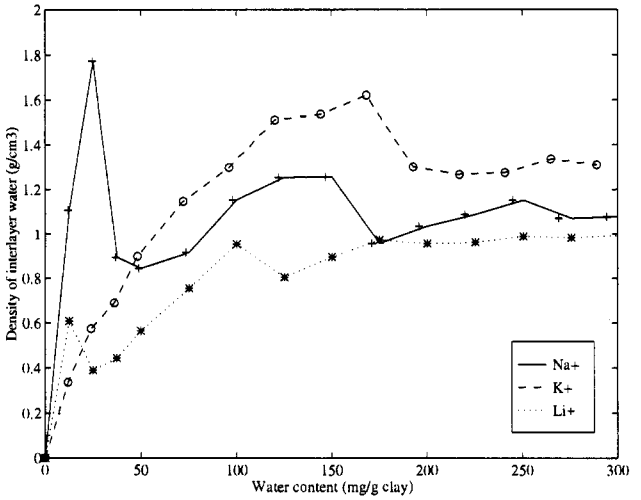

Figure 7. Density of interlayer water in Na^+-, Li^+-, and K^+-Wyoming montmorillonites as a function of increasing water content, compared to the anhydrous state.

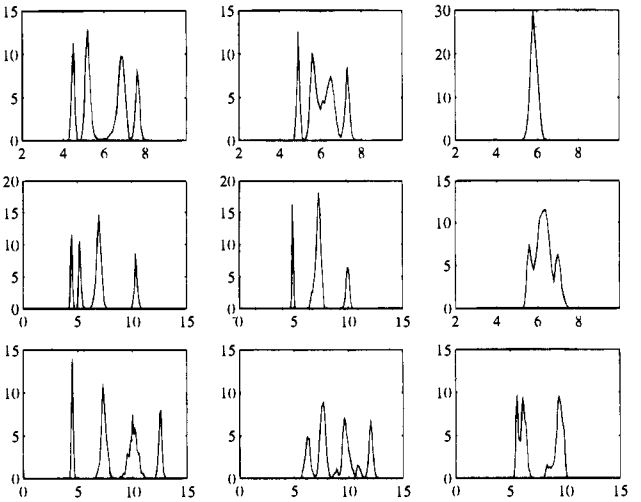

Figure 8. Density profiles for Li^+, Na^+, and K^+ counterions, in the first, second, and third columns, respectively. The water content increases from 32 molecules, 64 (for K^+ 56), to 96 water molecules, in the first, second, and third rows, respectively. Densities are measured as a function of the distance z (Å).

hydrate containing N water molecules and the anhydrous smectite and m_{H_2O} is the mass of a water molecule. These curves are presented in Figure 7. For the sodium case, it shows that the density increases steeply up to eight water molecules. In the next section it will be shown that the water molecules in this hydration stage are oriented coplanar with the clay layer. This may account for the high initial density. Then the density drops and slowly builds up again up to 48 H_2O molecules, when the first water layer is completed. Then the density drops and rises a bit again to accommodate the second water layer. The general trend is that the density converges slowly to the bulk water value of 1 g/cm^3. More or less the same trends are found for the Li-smectite: steps occur in the density profile in connection with the start of new water layers and at an earlier stage than for Na-smectite. For potassium, a different picture arises: the density increases slowly, without steps, up to 56 water molecules, where the first water layer is completed. Then the density drops, but remains significantly higher than the bulk water density. Potassium ions are known to break the water structure.[51] Therefore the local water density in the K-smectite may be higher than the bulk water density due to the presence of the potassium ions. As our calculated layer spacings agree well with the experimental ones, we may expect that this increased density is not a simulation artifact. It may be expected that, for higher water contents, the density will decrease asymptotically to the bulk water density.

3.2. Interlayer Molecular Structure. Having verified the thermodynamic properties of the smectite hydrates, and therefore the validity of the potential functions used, it is now justified to study the microscopic interlayer structure. First the distributions of the counterions are calculated, then the microscopic water structure is investigated.

3.2.1. Counterion Distributions. For all three ionic species, Li, Na, and K, the distribution of the cations was calculated as a function of the distance z, measured perpendicular to the midplane of the smectite (octahedral) layer. The cation densities of the three smectites are shown in Figure 8 for some representative stages of hydration. It should be kept in mind that the lower clay sheet remains fixed at the z-coordinate origin upon swelling, having surface tetrahedral oxygens at $z = 3.28$ Å. The upper clay layer moves toward higher values of z when the water content increases. Only the cations near the upper clay sheets are therefore subject to fluctuations of the interlayer spacing. This sometimes causes artificial asymmetry in the density profiles in Figure 8, *i.e.*, the density peaks on the left-hand side may be sharper than the ones on the right-hand side.

For both sodium and lithium, the trends emerging from these calculations show the same general features. At low water content (0−8 molecules) only one cation layer is present, splitting up into two parts upon further hydration. We refer to the cation densities for 32 water molecules in Figure 8. The first part is an "inner-sphere" surface complex,[35] consisting of (on the average) two ions, strongly bound to the tetrahedral substitution sites. The second part is an "outer-sphere" surface complex, consisting of four ions more loosely associated with the octahedral substitution sites. These ions are distributed roughly equally in two planes offset from the interlayer midplane. These results are in agreement with those of Skipper *et al.*[27] but slightly different from Chang *et al.*,[28] who found a third adsorbed species in their simulations of Na-smectites by using different force fields (MCY water and clay oxygen atoms instead of TIP4P). When the water content increases above 48 molecules, the inner-sphere complex persists, but the two outer-sphere complex layers collapse into one, more diffuse, ion layer which is highly solvated and resides in the midplane region (Figure 8). Presumably this layer is stabilized by the surrounding water bilayer, which is just forming at this stage (see next section). When the water content is increased above 80 molecules, this central layer splits up into several peaks, possibly related to the start of a "diffuse ion swarm" (Figure 8). A snapshot of this stage is presented in Figure 1.

For the potassium ion, the general picture is different from the Na^+ and Li^+ ions. From 0 to 48 water molecules in the interlayer spacing, the 6 K^+ ions remain in a single layer in the midplane region (Figure 8). In the anhydrous K-smectite, the K^+ ions are locked into the hexagonal surface cavities. As soon as the clay opens up, due to insertion of water molecules, the potassium ions move to sites above SiO_4 tetrahedra, rather than staying in the siloxane hexagonal cavities, as suggested by Sposito.[35] Indeed, a recent AFM study of interfaces between freshly cleaved muscovite mica and aqueous solutions[52] has shown that potassium ions could not reside in hexagonal cavities.

(51) Skipper, N. T.; Neilson, G. W. *J. Phys.: Condens. Matter.* **1989**, *1*, 4141−4154.

(52) Nishimura, S.; Biggs, S.; Scales, P. J.; Healy, T. W.; Tsunematsu, K.; Tateyama, T. *Langmuir* **1994**, *10*, 4554−4559.

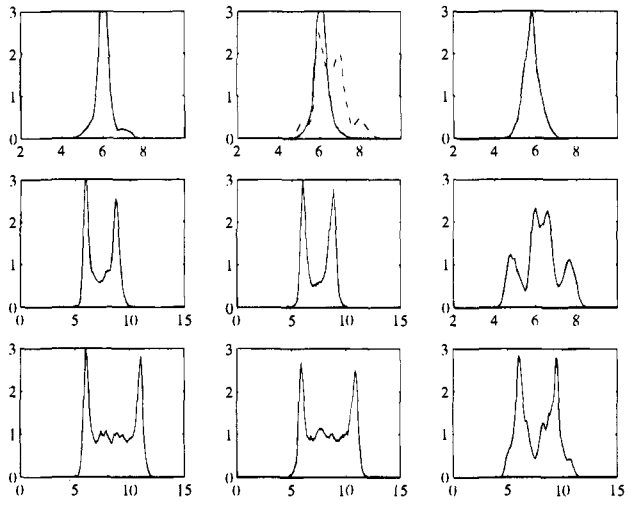

Figure 9. Density profiles for water molecules (oxygen atoms) in Li^+-, Na^+-, and K^+-montmorillonite hydrates, in first, second, and third columns, respectively. The water content increases from 32 molecules (for Na^+ also 48, dashed), 64 (for K^+ 56), to 96 water molecules, in the first, second, and third rows, respectively. Densities are measured as a function of the distance z (Å).

Our study confirms these experimental results. At a total of 56 water molecules, the single K^+ ion layer starts to split (Figure 8). Upon further hydration (up to 96 water molecules), a cation bilayer is formed, located close to the siloxane surfaces without water molecules interposed (Figure 8). At the beginning of the simulation runs all the cations are located at random near the midplane of the interlayer spacing. During the equilibration the cations are allowed to desolvate and indeed appear to end up at the surface. As there is no overlap between the two cation populations (Figure 8), the K^+ ions, once bound to the surface, do not solvate again. Therefore we conclude that K^+ ions are preferably bound to the clay surface. A simulation snapshot, presented in Figure 2, confirms this picture. In previous simulations, the potassium cation was moved together with the water molecules in its first solvation sphere as a whole, in one MC step.[32] This would seem inconsistent with the result that potassium ions, adsorbed on the surface, are only partially hydrated. In our simulations, the water molecules and cations are moved separately. In bulk aqueous solutions, potassium ions hydrate to a lesser extent than sodium and lithium ions do.[51] In smectite hydrates, we observe the same trend; the potassium ions are reluctant to form a full hydration shell and prefer to bind to the clay surface. This effect will reduce the tendency of K^+ saturated smectites to expand.

3.2.2. Interlayer Water Structure. In this section, the distribution of the water molecules is calculated from averaged coordinate data of the oxygen atoms of the water molecules. Several representative stages of hydration are shown in Figure 9. Second, average orientations of the water molecules are presented, calculated with respect to the clay surfaces.

The sodium and lithium smectites display the same qualitative features when the water density profiles are considered. As we go from 4 to 40 water molecules, the water monolayer in the interlayer spacing builds up, giving rise to one single peak in the density profile (see Figure 9). Then an instability is reached upon further increase of the water content, for both lithium (at 40 molecules) and sodium (at 48 molecules): at these points, the layer spacing keeps fluctuating strongly after 2 million steps of equilibration and the system seems to be unable to decide whether to adopt a monolayer or bilayer arrangement (Figure 9). Beyond this point, there is a clear water bilayer, building up between 48 and 80 water molecules and accommodating the central ion layer. Finally, for 88 and 96 molecules, the start of a third layer can be observed, more diffusely arranged around the midplane (Figure 9). Possibly it is related to the development of a diffuse ion swarm. Delville's simulations of Na-smectite[31] show that the transition from a one- to two-layer situation takes place at a somewhat larger layer spacing, possibly due to a different choice for the Na potential parameters. The same holds for the transition to a three-layer stage.

For the potassium smectite, the situation is different: at low water content (up to 24 water molecules) one central peak is present, slightly split up to accommodate the potasium ion layer, which turns into a single peak upon further hydration (Figure 9). Then there is a transition region where the central peak shows two satellite wing peaks (around 48–56 water molecules, Figure 9). This region is broader than for Na and Li and is followed by a definite two-layer stage beyond 64 molecules. This stage persists up to 96 molecules, and no incipient third water layer is observed.

For all three types of cations, the orientations of the interlayer water molecules go through three stages with increasing water content. At a low degree of hydration (4 to 8 molecules), the water molecules tend to be "squeezed" in a flat orientation, coplanar with the confining clay surfaces. In this way the contact area with the clay is maximized, and the interaction energy is minimized. This provides a likely explanation for the experimental difficulties in removing the last water molecules from a clay upon dehydration.[50] By increasing the number of water molecules, the monolayer gets filled up and the measured H–H vector distribution shows a preference for orientations perpendicular to the clay surface. Initially, the water molecules orient themselves with their dipole moments parallel to the clay surface. With increasing water content (up to 40 molecules) the dipole moments gradually rotate such that half of the O–H vectors of the water molecules are perpendicular to the clay surface, forming hydrogen bonds with the surface oxygens of the siloxane surfaces. In contrast with the results of Chang *et al.*,[28] we find that this transition takes place well before the formation of a bilayer. When the number of water molecules is increased above 56, a two-layer hydrate originates. In this situation a water molecule forms one hydrogen bond with the clay surface, the other O–H bond being involved in hydrogen bonding with neighboring water molecules. This can be observed from the images presented in Figures 1 and 2.

4. Conclusions

We have investigated the microscopic mechanisms underlying the swelling of Li-, Na-, and K-Wyoming montmorillonites by means of Monte Carlo simulations. As the water content is increased systematically from 0 to 0.3 g/g of clay, both the Na^+ and Li^+ ions hydrate in the interlamellar spacing, thereby forcing the clay layers apart in a series of discrete steps. The agreement found between simulation data for the clay layer spacing and experimental swelling curves is remarkable. The experimental curves show hysteresis loops upon contraction or expansion. Intriguingly, these loops enclose our calculated data. The general accuracy of these results reflects the quality of the interaction potentials employed. Focusing on the microscopic interlayer structure, we observe that, upon hydration, the Na^+ and Li^+ ions become detached from the surface and form a diffuse ion swarm. The K^+ ions on the other hand migrate to and then remain bound to the clay surface, reluctant to hydrate. This effect reduces the tendency of K^+-saturated clays to expand, as the K^+ ions screen the negatively charged, mutually repelling clay surfaces more effectively than Na^+ and Li^+ ions

do. This provides an explanation at the molecular level for the shale-swelling inhibition properties of K^+ ions. The latter result bears relevance to the oilfield interest in understanding clay swelling: having established the fundamental molecular mechanisms for clay swelling and inhibition, it should be possible to design novel shale stabilizers, which include both ionic and polymeric species. In this paper, we have introduced a new set of interaction potentials, which will lend themselves to the incorporation of intercalated organic molecules. In subsequent papers, we shall describe a complementary molecular-dynamics simulation study of transport properties in smectite hydrates[53] and a study of organic shale inhibitors.[54]

We believe that the differences our simulations have uncovered between sodium and potassium ions within clays probably extend to the wider field of colloid science and indeed also to physiology. In both these areas, the role played by sodium and potassium ions is quite distinct and is a reflection of the affinity of each ion for a surface or a binding protein, compared with the tendency of the ion to hydrate.[17,55]

Acknowledgment. We are grateful to Bernadette Craster, Jane Denyer, Henk Lekkerkerker, Geoff Maitland, Paul Reid, Paul van der Schoot, and John Sherwood for helpful discussions during the course of this work.

JA952139T

(53) Boek, E. S.; Coveney, P. V., in preparation.

(54) Bains, A.; Boek, E. S.; Coveney, P. V., in preparation.

(55) Hille, B. *Ionic Channels of Excitable Membranes*; Sinnauer Associates Inc.: Sunderland, MA, 1984.

(56) Boek, E. S.; Coveney, P. V.; Skipper, N. T. *Langmuir* **1995**, *11*, 4629–4631.